FEATURE ARTICLE

Ru-Decorated Pt Surfaces as Model Fuel Cell Electrocatalysts for CO Electrooxidation

F. Maillard,[†,‡] G.-Q. Lu,[§] A. Wieckowski,*[,§] and U. Stimming*[,‡]

Laboratoire d'Electrochimie et de Physicochimie des Matériaux et des Interfaces, UMR CNRS 5631, ENSEEG, BP75, 38402 Saint Martin d'Hères, France, Department of Physics E19, Technische Universität München, James-Franck-Str. 1, D-85748 Garching, Germany, and Department of Chemistry, University of Illinois at Urbana-Champaign, Urbana, Illinois 61801

Received: May 2, 2005; In Final Form: June 10, 2005

This feature article concerns Pt surfaces modified (decorated) by ruthenium as model fuel cell electrocatalysts for electrooxidation processes. This work reveals the role of ruthenium promoters in enhancing electrocatalytic activity toward organic fuels for fuel cells, and it particularly concerns the methanol decomposition product, surface CO. A special focus is on surface mobility of the CO as it is catalytically oxidized to CO_2. Different methods used to prepare Ru-decorated Pt single crystal surfaces as well as Ru-decorated Pt nanoparticles are reviewed, and the methods of characterization and testing of their activity are discussed. The focus is on the origin of peak splitting involved in the voltammetric electrooxidation of CO on Ru-decorated Pt surfaces, and on the interpretative consequences of the splitting for single crystal and nanoparticle Pt/Ru bimetallic surfaces. Apparently, screening through the literature allows formulating several models of the CO stripping reaction, and the validity of these models is discussed. Major efforts are made in this article to compare the results reported by the Urbana-Champaign group and the Munich group, but also by other groups. As electrocatalysis is progressively more and more driven by theory, our review of the experimental findings may serve to summarize the state of the art and clarify the roads ahead. Future studies will deal with highly dispersed and reactive nanoscale surfaces and other more advanced catalytic materials for fuel cell catalysis and related energy applications. It is expected that the metal/metal and metal/substrate interactions will be increasingly investigated on atomic and electronic levels, with likewise increasing participation of theory, and the structure and reactivity of various monolayer catalytic systems involving more than two metals (that is ternary and quaternary systems) will be interrogated.

I. Introduction

Pt-based electrodes are commonly used as electrocatalysts for low temperature fuel cells. However, in the electrooxidation reactions occurring at the fuel cell anode, adsorbed CO poisons the catalyst surface and significantly reduces the fuel cell performance. As is well-known, the addition of Ru to Pt increases the "CO-tolerance" of platinum in direct methanol oxidation fuel cells (DMFCs) or, more generally, in polymer electrolyte membrane fuel cells (PEMFCs). The origin of such an enhancement has been a subject of many studies but still remains an incompletely resolved issue. Within the ligand effect approximation, addition of Ru increases CO tolerance via electronic interactions that may cause, for instance, the reduction in the Pt−CO bond strength, which may facilitate CO oxidation.[1−3] On the other hand, within the realm of a bifunctional mechanism,[4,5] it is assumed that Ru provides an oxygenated surface species by dissociating water at the Ru sites at lower potentials against pure Pt sites, leading to the accelerated CO_2 formation and a decrease in the CO poisoning, thus improving the CO tolerance. Several groups have investigated the origin of the Ru enhancement by using various types of model bimetallic Pt/Ru electrodes, including Pt/Ru alloy[6−14] and Ru-decorated Pt electrodes.[1,4,14−42] Although the structure of the latter may, in principle, differ considerably from that of the Pt/Ru alloys, studying electrocatalytic activity on the Ru-decorated Pt surfaces for CO electrooxidation is an essential step in obtaining a general understanding of fuel oxidation mechanisms on Pt/Ru surfaces.

Recently, Babu et al.[43,44] have reported that surfaces of Pt/Ru alloy nanoparticles are strongly Pt enriched. It was also found that the increase in the temperature increased the Pt/Ru nanoparticle size and changed the layered composition of the Pt/Ru nanoparticles in terms of the ratio of Pt to Ru across the nanoparticles.[44] The data also indicate that in the Pt/Ru alloy, Ru is present on the nanoparticle surface,[43] forming platinum enriched Pt/Ru layers,[44] and the Pt/Ru alloy nanoparticle catalyst is—under fuel cell operation conditions—equivalent to that produced by the Ru decoration tactics. Interestingly, Maillard et al.[21] found enhanced kinetics for methanol electrooxidation on the Ru-decorated Pt nanoparticles compared to the Pt/Ru alloy. Similarly, Dubau et al.[45] observed that for the same Pt/

* Corresponding authors. E-mail: Ulrich_Stimming@ph.tum.de; andrzej@scs.uiuc.edu

† Laboratoire d'Electrochimie et de Physicochimie des Matériaux et des Interfaces.

‡ Technische Universität München.

§ University of Illinois at Urbana-Champaign.

10.1021/jp052277x CCC: $30.25
Published on Web 08/05/2005

Frédéric Maillard received his M.Sc. in 1999 from the I.N.P.Grenoble, France, and his Ph.D. in Physical Chemistry from the University of Poitiers, France, in 2002. After two years of postdoctoral work with Prof. U. Stimming and Dr. E. Savinova at the T. U. München, Germany, he became a CNRS scientist in 2005 at the L.E.P.M.I. in Grenoble. His research interests are electrocatalysis with fuel cell materials, notably nanoparticles, and in-situ electrochemical methods (FTIR, EQCM, STM).

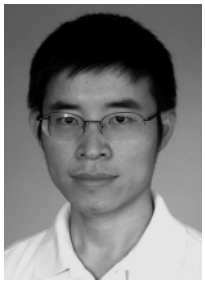

Guo-Qiang Lu received his B.S. degree in Chemistry in 1992 and his Ph.D. in 1997, both from Xiamen University, China. He is currently a visiting research associate in University of Illinois at Urbana-Champaign. His research interests are in spectroelectrochemistry and electrocatalysis, focusing on in-situ sum frequency generation on platinum electrodes and bimetallic electrodes.

Andrzej Wieckowski is Professor of Chemistry at the University of Illinois at Urbana-Champaign, Illinois, and North American Editor for *Electrochimica Acta*. He received his Ph.D. and D.Sc. in 1981 from University of Warsaw, Poland. Wieckowski pioneered the development of electrochemical NMR (EC-NMR), which combines metal/surface NMR and electrochemistry for studies of electrochemical interfaces. His group contribution is through new catalyst syntheses, the use of electroanalytical and spectroscopic methods (EC-NMR, XPS, STM, SFG) and synchrotron methods for single crystal and nanoparticle studies, and through broadly publicized correlations of electronic-level data and reactivity for fuel cells.

Ulrich Stimming is currently a Professor of Physics and Chemistry, Dept. of Physics E19, Interfaces and Energy Conversion, at the Technical University of Munich, Germany. He is a member of the Board of directors of the Bavarian Center of Applied Energy Research, ZAE Bayern. He has received his Ph.D. in Physical Chemistry from the Free University of Berlin; Germany. Previously, he has held faculty positions at Columbia University in New York and at the University of Bonn, Germany. He also was a director at the Research Center of Jülich where he set up a broad-range fuel cell research program. Prof. Stimming is Editor-in-Chief of the journal *Fuel Cells - From Fundamentals to Systems* published by Wiley-VCH.

Ru ratio, a mixture of Pt and Ru colloids supported on Vulcan displayed enhanced kinetics for both CO and methanol (MeOH) electrooxidation as compared to the Pt/Ru alloys. Thus, an alloy formation is not a prerequisite for obtaining effective CO-tolerant electrocatalysts, but the Pt and Ru atoms have to be in close proximity to act catalytically for the CO removal from the surface.[19−21,45]

Concerning the preparation of the Ru modified Pt electrodes, literature data indicate that spontaneous deposition of ruthenium,[20,21,23−33,46,47] as well as electrodeposition,[16−21] metal vapor deposition,[36−40,48] and surface organometallic chemistry[49−51] are all suitable methods to produce two-dimensional (2D) nanosized and catalytically active Ru islands dispersed on many types of supported or unsupported Pt substrates. Access to the morphology and coverage of such systems is possible through the methods such as: in situ scanning tunneling microscopy (STM), low electron energy diffraction (LEED), X-ray methods and Auger electron spectroscopy (AES), which provide powerful tools to establish the link between the surface structure and electrocatalytic activity. Major studies in the CO monolayer electrooxidation were performed by Friedrich et al.[17−19,52,53] and Chrzanowski et al.[24−26,54] on the Ru-decorated Pt(111) surfaces using electrochemical and spontaneous deposition schemes, respectively. However, the mechanism of the CO electrooxidation on these surfaces is not yet clear. Indeed, whereas on the Ru-decorated Pt(111) surface Friedrich et al.[19] observed a single CO stripping peak shifted negatively compared to the position of CO electrooxidation on pure Pt(111), a double or split peak behavior was reported by Massong et al.[42] and then confirmed by Lu et al.[33] and Davies et al.[40] Further, Bergens et al.[50,55] Waszczuk et al.[30] and Maillard et al.[20] obtained the split peak for CO oxidation on Ru-decorated Pt nanoparticles. In parallel (or subsequently), in situ Fourier transformed infrared (FTIR),[16−20,46,56] sum frequency generation (SFG)[57] and electrochemical nuclear magnetic resonance (EC NMR)[3,31] spectroscopies were used to probe the nature of the binding site and the binding mode of the CO on these types of surfaces. Two CO populations were identified on the Ru-decorated Pt(111) electrodes[17,57] and Ru-decorated Pt nanoparticle electrodes:[20] CO adsorbed on the Ru sites and CO adsorbed on the Pt sites. Massong et al.[41] found that CO adsorbed in the vicinity of the Ru adislands was electronically affected, whereas the CO adsorbed at Pt sites far away from Ru sites was not affected. Slow diffusion for CO was suggested as the origin of the two-peak behavior.[58] An alternative explanation was suggested to be the low reactivity at the Pt/Ru edge.[33]

The issues summarized above are those that we want to address in this paper. We will review different methods used to prepare Ru-decorated Pt single-crystal surfaces as well as Ru-decorated Pt nanoparticles, and we will demonstrate how to characterize them and to test their activity for the model CO monolayer electrooxidation. A special effort will be made to compare the results reported by the Urbana-Champaign group

and the Munich group, but also by others. We will focus on the origin of the peak splitting in the CO oxidative voltammetry on Ru-decorated Pt surfaces and, in this electrochemical context, explore surface reactivity models that so far have been developed, and discuss their validity.

II. Preparation and Characterization of Ru-Decorated Surfaces

II.1. Decoration of Pt Surfaces by Electrochemical Deposition. In 1975, Watanabe and Motoo pioneered the modification of a Pt surface by Ru adatoms by the use of electrodeposition. They observed a pronounced enhancement in the electrooxidation kinetics of both carbon monoxide and methanol.[4] Focusing next on single-crystal electrodes, a repeated cycling in the $RuCl_3$ containing solution was used to modify Pt(110) and Pt(111) surfaces by ruthenium.[22] However, due to the low current efficiency of Ru electrodeposition under such conditions,[21,25,26,35,59] potential steps were utilized in order to facilitate the process of addition of Ru to Pt single-crystal surfaces,[16,18,26] polycrystalline Pt,[35,59] or to Pt nanoparticles.[21] Friedrich et al. highlighted the most promising conditions for the Ru electrodeposition.[18] For the electrode potential more positive than 0.9 V vs RHE, no Ru deposition was observed as inferred from cyclic voltammetric measurements. In the potential range of $0.3\ V \leq E \leq 0.8\ V$ vs RHE, submonolayer amounts of Ru were formed, and the Ru surface coverage was increasing linearly with the decreasing potential,[18] or with the increase in the electrolysis time,[21] whereas at potentials below 0.25 V vs RHE, a massive nucleation and growth of Ru metal occurs.[18]

Electrochemical quartz microbalance (EQCM) experiments at a quartz crystal supported Pt electrode allowed monitoring of the extent of electrodeposited Ru.[21,35,59] It was noted that the variation of Δm with t became almost negligible for large times, suggesting a significant drop of the electrolysis yield. This observation was confirmed by AES[25] and electrochemical studies,[26,54] using single-crystal electrodes. The decrease of the electrolysis yield was attributed to an auto-inhibitive influence of Cl^- ions, which are produced at the interface in the course of $RuCl_3$ electroreduction, and adsorb strongly at the electrode surface. However, Maillard et al., using a $Ru(NO)(NO_3)_3$ salt and a nonadsorbing electrolyte ($HClO_4$), observed a similar effect.[21] Therefore, these observations are a strong indication that the formation of Ru oxides/hydroxides, which inhibit further Ru growth, is more likely involved.[21]

Cramm et al. also pioneered the STM imaging of Ru-modified Pt surfaces in an in situ STM cell (see Figure 1).[16] Evidence was provided for formation of commensurate Ru islands, 2−5 nm large on Pt(111), in which island size did not depend on the deposition potential. These islands were proved to be mainly monatomic. (The tendency to form a bilayer configuration at about 10% of the total Ru coverage was later pointed out by Herrero et al.)[23] Further, X-ray diffraction (XRD)[60] and reflection high energy electron diffraction (RHEED)[13] measurements proved that the Ru deposits on Pt(100) and Pt(111) displayed a commensurate (1×1) structure. Notice that Ru electrodeposition on Pt(111) proceeds via Volmer−Weber growth as a bilayer configuration was detected by RHEED for Ru coverages larger than 0.4 ML.[13] Interestingly, there is no preferential deposition of Ru on surface steps under both electrodeposition[16] and spontaneous deposition[28,32,61] conditions, indicating that the Ru nucleation does not occur preferentially at crystallographic defects, and that the Ru islands are randomly dispersed over the electrode surface. This is a very important conclusion because it discards the possibility of Ru to promote CO electrooxidation kinetics by blocking active Pt sites for CO adsorption, water dissociation, or other related surface events.

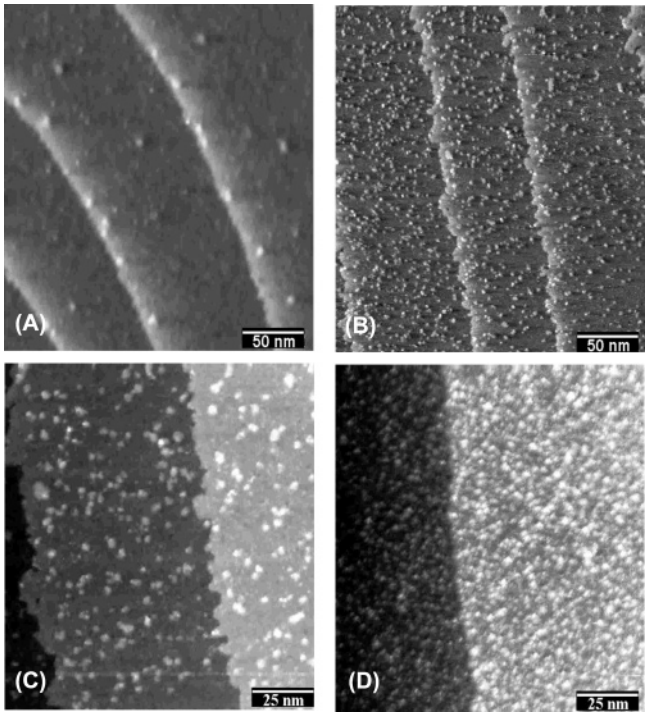

Figure 1. STM images of Ru-modified Pt(111) electrodes recorded in 0.1 M $HClO_4$ at 0.5 V vs RHE. (A) Substrate without CO. (B) Deposition was performed prior to imaging in a standard glass cell from 0.1 M H_2SO_4 + 5 mM $RuCl_3$ at 0.6 V vs RHE for 5 min. (C) Higher resolution image of surface in (B). (D) Deposition was performed for 30 min. (Reprinted with permission from ref 19.)

Pt nanoparticles can also be decorated by Ru using both spontaneous[21,30] and electrochemical depositions,[20,21] similarly to what was done on Pt single crystals. Because the STM, LEED, LEIS (low energy ion scattering), and AES experiments are difficult to carry out on nanoparticles, very little is known about the structural characteristics of these nanoparticle deposits, and more work is necessary. However, these decoration approaches are important in order to compare a broad range of industrial catalysts to those obtained in the laboratory and allow for the study the Ru coverage and particle size effects as they depend on the catalyst pretreatment or physical and chemical properties of the nanoparticle (carbon) support.

II.2. Decoration of Pt Surfaces by Spontaneous Deposition. Janssen and Moolhuysen studied a large number of platinum based binary catalysts prepared by the deposition of submonolayer amounts of the second components without the use of electrical current (the so-called "immersion method") onto hydrogen covered surfaces of platinum.[15] They reported a pronounced activity for methanol oxidation on the ruthenium- and titanium-decorated Pt surfaces. The decoration of Pt single crystals by spontaneous deposition of ruthenium (without the hydrogen preadsorption) was first reported by Chrzanowski et al.[24,25] (recently reviewed in ref 62). Such a spontaneous deposition is carried out at an open circuit potential by immersing a Pt electrode for different periods in the N_2-purged 0.1 M $HClO_4$ containing $RuCl_3$ solutions.[24−26] Note that aging of the solution for 2−3 weeks is necessary to obtain solutions containing hydrated Ru^{IV} complexes needed for a successful spontaneous deposition experiment. The spontaneous deposition[24] is proposed to occur according to reaction 1, while further electroreduction of the Ru containing deposit begins according to reactions 2 and 3, followed by a complete reduction of the

Ru oxides to metallic ruthenium:[63]

$$[RuO(H_2O)_4]^{2+} \rightarrow RuO_{2ads} + 3H_2O + 2H^+ \quad (1)$$

$$RuO_{2ads} + 2H^+ + 2e^- \rightarrow RuO_{ads} + H_2O \quad (2)$$

$$[RuO(H_2O)_4]^{2+} + A^- + e^- \rightarrow RuO_{ads} + A_{ads} + 4H_2O \quad (3)$$

The complementary redox to reaction 1 could then be the oxidation of the platinum surface:

$$Pt + xH_2O \rightarrow PtO_xH_y + (2 - y)H^+ + (2x - y)e^- \quad (4)$$

and reactions 3 would explain the high open circuit potential (>800 mV) observed during the deposition process on Pt(*hkl*) surfaces,[24] and on unsupported and carbon-supported Pt nanoparticles.[21,30] Similarly, Clavilier and Feliu demonstrated that arsenic and antimony compounds[64] as well as bismuth[65] could be irreversibly adsorbed from acidic solutions on Pt(*hkl*).

The coverage of spontaneously deposited Ru on Pt depends on the Pt crystallographic orientation and is higher on Pt(100) than on the other low index Pt planes, suggesting a site geometry sensitive electrochemical process.[24] As adsorption time or the Ru concentration in the electrolytic bath is increased, an increase in the Ru coverage is found.[21,25] However, from a single spontaneous deposition, a maximum ruthenium coverage is no higher than 20%, both on Pt(*hkl*) surfaces[26] and on Pt nanoparticles.[21] This might be related to steric reasons, the presence of Cl^- ions coming from the $RuCl_3$ salt, and/or to the presence of nonreducible Ru oxides in the spontaneous deposit. However, chloride anions were never found when the Pt/Ru surfaces were transferred from the electrochemical cell to UHV after the deposition. Indeed, the spontaneous deposition leads to a mixture of Ru oxides (hydroxides) on the Pt surface,[26,66] which is not fully reduced by an extended polarization at 0.3 V vs RHE or by cyclic voltammetry.[29] This is likely the reason several cyclic voltammetric cycles in a full electrode potential range (from hydrogen evolution to oxide formation on platinum) are necessary to "stabilize" the electrode electrochemical behavior of such Pt/Ru surfaces.[23]

Similarly to the case of electrochemical deposition on Pt(111), Herrero et al.[23] found that the spontaneously obtained deposits were arranged in nanometer sized islands, with no preferential nucleation at the steps. The island appeared to be round shaped, except when they collapsed to form bigger islands. Interestingly, while most of the islands were monatomic, a fraction of the islands, approximately 10% of the total ruthenium coverage, displayed a second monolayer deposit over the first monolayer. This is actually the major difference with Ru islands formed by electrochemical deposition, where up to 0.7 monolayer of Ru on Pt could be reached with monatomic Ru islands.[16] Crown,[32] Hoster,[37] and then Waszczuk[30] and collaborators demonstrated that a larger Ru coverage on Pt(*hkl*) could be obtained by a "repeated spontaneous deposition".[32,67] Notably, the single spontaneous deposition is a surface structure sensitive reaction as the details of the islands growth depend strongly on the type of the crystal Pt(*hkl*) plane used. For instance, on Pt(111), after four depositions, approximately 30−35% of the surface is covered by Ru, 65% of the islands being monatomic, 25% consist of two Ru layers, and 10% of three Ru layers. As a consequence, for electrodes obtained by the repeated spontaneous deposition process, the Ru packing density rather than the Ru coverage should be used. If monatomic islands are formed on the surface, these two quantities are equal. If the repeated spontaneous deposition is used, then the Ru coverage is always smaller than the Ru packing density.

Very little is known about the structure of Ru islands on Pt nanoparticles after the (repeated) spontaneous deposition; it is assumed that the deposition occurs on Pt nanoparticles as on Pt(*hkl*) surfaces. A systematic characterization of Ru spontaneous deposition processes on Pt nanoparticles is therefore necessary.

II.3. Decoration of Pt Surfaces under UHV Conditions. The UHV environment allows cleaning and ordering of the Pt (substrate) surfaces using ion bombardment, chemical reactions, and annealing.[54] Ru submonolayers can be prepared using metal vapor deposition,[14,36−40] characterized with electronic diffraction methods, STM or XPS (X-ray photoelectron spectroscopy),[38−40,63] and transferred (back and forth) to the electrochemical environment.[14] The main advantage of these techniques is that thermal treatment in a broad temperature range can be applied to process platinum single-crystal electrodes modified with Ru[14,37−40] or to form Pt/Ru subsurface alloys after annealing the Ru-decorated Pt surfaces in a truly clean environment.[14,37,38] The access to the powerful UHV characterization techniques, including real time characterization during vacuum deposition runs, is noteworthy.[24,25] Davies et al.[38] using LEIS and XPS, reported that Ru deposited at 300 K by metal vapor deposition on a Pt(110) surface is incorporated in the second or third layer if the surface is annealed over a wide temperature range (350−1000 K). Jarvi et al.[36] using Auger spectroscopy reported a 10% decrease in the ruthenium 273 eV peak-to-peak height after annealing at 600 K in vacuum of the Ru-decorated Pt(111) surface (θ_{Ru} = 0.28 ML), confirming the formation of a surface alloy and also the fact that Ru remains in the subsurface region. Similar study concerning electrochemically deposited Ru should also be noted.[25]

Apparently, evaporation of Ru onto the Pt(111) surface leads to formation of Ru islands having a width of 2−10 nm[14] depending on the Ru coverage. As expected, steps act as the preferential nucleation centers for the Ru growth and, interestingly, they provide nucleation centers on both parts of the terrace i.e., the steps are decorated from both sides.[14] Some evidence of Ru clustering on Pt(110) after metal vapor deposition at 300 K was found.[37,38] Here, the second layer starts to form on top of Ru islands before the first one is complete[13] (the Volmer−Weber growth mode) due to the strain caused by a slight lattice misfit between Pt and Ru (also observed in the case of spontaneous deposition).[23] The difference in surface energy of Pt vs Ru is more significant than the lattice mismatch. Notably, when grown at higher temperatures, Ru islands tend to form a bilayer configuration.[14]

II.4. Organometallic Decoration of Pt Surfaces with Ru Adatoms. One possible decoration technique that is notable is surface organometallic chemistry (SOMC), a technique which engineers Pt nanoparticles covered by organometallic precursor of Ru.[49,55] Lee et al. deposited Ru adatoms on rough (black) Pt gauze by hydrogenation of organometallic compounds [Ru(1,5-cyclooctadiene)(eta(3)-C3H5)(2)] dissolved in hexanes solution.[55,68,69] The deposition was carried out at a low temperature under 1 atm of hydrogen. A series of Pt/Ru surfaces were prepared by interrupting the hydrogenation after deposition of 0.05, 0.10, 0.30, 0.32, 0.44, 0.70, and 3.5 equivalent of Ru adatoms. The amount of Ru deposited on Pt could be determined from either the amount of [Ru(1,5-cyclooctadiene)(allyl)2] consumed, from the amount of cyclooctane produced, or by exhaustive anodic stripping of the Ru adatoms from the resulting

Pt/Ru surfaces followed by ICP analysis of the electrolyte for Ru ions. Stripping voltammetry of adsorbed monolayers of carbon monoxide from these surfaces showed a drop by 120 mV in the CO stripping peak potential upon deposition of 0.05 equivalent of Ru adatoms on Pt. Such surfaces were evaluated as catalysts for the electrooxidation of methanol. The measured currents were normalized to the specific surface areas of the gauzes measured before deposition of Ru adatoms. The order of activity of the CO-poisoned Pt/Ru surfaces toward potentiodynamic oxidation of methanol (0.5 M H_2SO_4) was 0.05 > 0.10 > 0.30 ≈ 0.44 > 0.7 > 0 (Pt) equivalent of Ru adatoms (0.5 M H_2SO_4, sweep range 0.025−0.60 V, sweep rate 5 mV/s, 25 °C). The activity of pure Pt increased relative to these other surfaces as the potential increased. Surfaces with low equivalents of Ru adatoms (from 0.05 to 0.10 equivalent) were the most active toward the potentiostatic oxidation of methanol with between 50 and 28 times higher turnover numbers than the black Pt. This is in very good agreement with the data reported by Maillard et al. at room temperature for Ru-decorated Pt nanoparticles.[21] In 0.5 M methanol solution in 0.5 M H_2SO_4, the activation energies for the oxidation of methanol over 0.05 and 0.10 equivalent of Pt−Ru-ad were 37 and 45 kJ/mol, respectively. These data are much lower than reported by other authors[26,70] but in very good agreement with the measurements of Dubau et al.[71] (30 kJ/mol for (80:20) Ru-decorated Pt nanoparticles.

Crabb et al.[51] prepared and characterized a series of Ru-modified Pt/C catalysts by SOMC (using ruthenocene, Cp_2Ru) with the nominal Ru:Pt surface ratios of 1:4, 1:2, 3:4, and 1:1. The XRD data showed no evidence of bulk PtRu alloying following the SOMC modification. Upon electrochemical reduction, EXAFS indicated a surface alloy formation. The CV studies show that the electrooxidation of CO on the Ru modified Pt/C occurs at lower potentials than on the unmodified catalysts, but at higher potentials than on a 1:1 bulk alloyed PtRu/C. Half-cell polarization measurements in H_2 containing 100 ppm CO show that the CO tolerance of the SOMC RuPt/C catalysts approached that of a conventional PtRu/C alloy catalyst. It was also found that higher Ru coverages increase both CO tolerance and CO electrooxidation activity.

II.5. Electrochemical Characterization of the Ru-Decorated Pt Surfaces. Typical cyclic voltammetric curves in a H_2SO_4 solution for the Ru-modified Pt(111) surfaces are presented in Figures 2 and 3. Increasing the Ru coverage leads to suppression of the long-range order characteristics in the voltammetry of Pt(111) associated with anion adsorption/desorption.[72] This is evidence that the Ru islands are uniformly dispersed on the surface, which also discards the possibility of having large (>100 nm^2) areas of unmodified Pt on the surface. For the Ru-decorated Pt(110) surface, the hydrogen adsorption/desorption features are clearly attenuated.[38] For high Ru coverage ($\theta_{Ru}^{LEISS} \geq 0.39$ monolayer, see Figure 2), new electrochemical features appear at 0.12 and 0.18 V vs RHE on the negative-going scan, that may be associated, in the first approximation, with hydrogen adsorption/desorption from Ru islands, as was reported on pure ruthenium electrodes[73] and on Ru-decorated Pt electrodes.[1,17,30,36,37,40] These electrochemical features disappeared when the surface was annealed to 600 K due to the migration of Ru into the near-surface layers. However, more recent work suggests they these peaks relate to OH adsorption/desorption on Ru(0001) at these potentials.[74,75]

The essential issue is to be able to accurately determine the Ru coverage on the noble metal substrates, starting with clean platinum. For alloys and nanoparticles, X-ray methods provide incomplete quantitative data since the measurements determine the amount of Ru not only on the surface but also in the bulk of the substrate.[12,76] This is in contrast to the decoration procedures where it is known that the Ru is on the substrate surface only. Thus, the above-mentioned surface sensitive methods, such as AES, LEIS, XPS, or in situ STM, have been used to quantify the Ru/Pt ratio and inform on the Ru oxidation states before or after the electrochemical experiments. On the other hand, attempts to quantify the Ru coverage by electrochemical methods have been proposed. Chrzanowski et al. found a linear relationship between Δ, the difference the voltammetric peak currents in the double layer range, and the Ru coverage

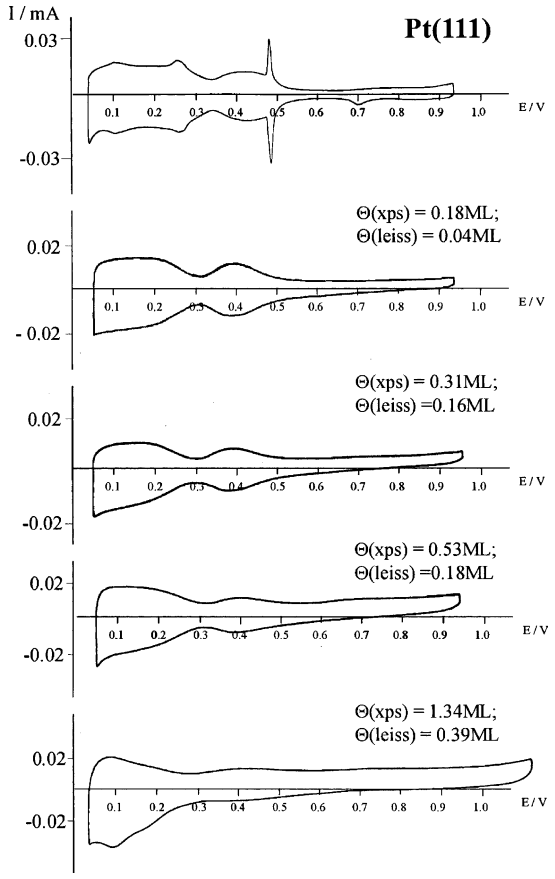

Figure 2. Cyclic voltammetry (0.5 M H_2SO_4, 100 mV s^{-1}) for clean and Ru-decorated Pt(111) surfaces. The ruthenium coverages measured using XPS (Θ_{XPS}) and LEISS (Θ_{LEISS}) before transfer to the electrochemical cell are indicated. (Reprinted with permission from ref 40.)

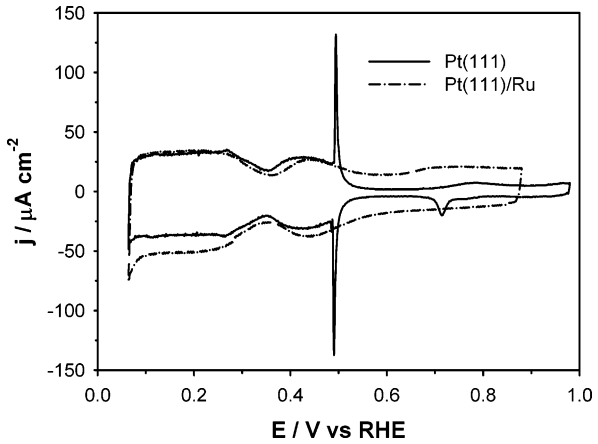

Figure 3. Cyclic voltammetry (0.1 M H_2SO_4, 50 mV s^{-1}) for clean and Ru-decorated (ca. 0.35 ML of Ru) Pt(111) surfaces. (Data from Urbana-Champaign.)

determined by AES.[24,25] In fact, for all Ru-modified Pt single crystals and nanoparticle surfaces, an increase in the double layer charging current (0.35−0.6 V) due to Ru addition was reported, due to the Ru oxide formation on Ru islands. By the combined AES and electrochemical measurements on Ru modified Pt-(111), Lin et al. have also shown that for the Ru modified Pt surfaces the double-layer charge measured in the potential range between 0.35 and 0.6 V increases linearly with the amount of Ru deposited.[13] These results are in good agreement with earlier suggestions by Watanabe and Motoo.[4] Using cyclic voltammetry (CV) coupled with electrochemical quartz-crystal microbalance (EQCM) experiments,[59] Frelink et al. showed that a linear relationship exists between the Ru coverage and the oxide reduction potential, thus allowing the Ru coverage to be measured on Pt. However, this method is destructive because the potential cycling up to the "oxide region" that is necessary irreversibly alters the electrocatalytic properties of the PtRu surface.

On the Ru-decorated Pt nanoparticles, additional experimental problems arise due to the large double layer capacitance induced by the high surface area carbon support. Thus, the coverage measurements based on the Ru redox currents in the double layer region are less accurate than for Pt(*hkl*) surfaces.[25] Maillard et al.[21] observed that the voltammetric peak-current at 0.12 V vs RHE (ascribed to the H desorption from Pt(110)-like sites) decreased with the increase in the Ru coverage (in the coverage range of 0 to 0.3). Then, the decrease in the plot of Ru coverage vs the peak height, denoted as δ, was found to exhibit a linear relationship and appeared to be a convenient tool for assessing the Ru coverage. However, this relationship is not valid for Ru coverages larger than 0.3 because of appearance of the electrochemical features at 0.12 and 0.14 V (vs RHE) associated with the redox process occurring on Ru islands (see above). The practical measure then to determine the composition of the uppermost layer of Ru-decorated Pt nanoparticles is to dissolve the particles in aqua regia and to determine the Pt/Ru ratio by the use of inductive coupled plasma (ICP).[30]

III. Electrocatalytic Activity of Ru-Decorated Pt Surfaces for CO Electrooxidation

III.1. Mechanism of CO Electrooxidation. On pure Ru and Pt surfaces, it is now generally accepted that the electrooxidation of adsorbed CO follows a Langmuir−Hinshelwood mechanism in which CO reacts with an oxygen-containing species present on the surface.[8] On Ru[8]

$$H_2O + Ru \rightarrow OH_{ads,Ru} + H^+ + e^- \quad (1)$$

$$CO_{ads,Ru} + OH_{ads,Ru} \rightarrow CO_2 + H^+ + e^- + 2{*}Ru \quad (2)$$

and on Pt

$$H_2O + Pt \rightarrow OH_{ads,Pt} + H^+ + e^- \quad (3)$$

$$CO_{ads,Pt} + OH_{ads,Pt} \rightarrow CO_2 + H^+ + e^- + 2{*}Pt \quad (4)$$

or, directly[77,78]

$$H_2O + Pt \rightarrow H_2O_{ads,Pt} \quad (3')$$

$$CO_{ads,Pt} + H_2O_{ads,Pt} \rightarrow CO_2 + H^+ + e^- + 2{*}Pt \quad (4')$$

Separately, on the Pt−Ru edge ("*" indicates the edge sites), where the bifunctional mechanism operates, the mechanisms most likely are[8]

$$H_2O + {*}Ru \rightarrow OH_{ads,Ru} + H^+ + e^- \quad (1)$$

$$H_2O + {*}Pt \rightarrow OH_{ads,Pt} + H^+ + e^- \quad (3)$$

$$CO_{ads,Ru} + OH_{ads,Pt} \rightarrow CO_2 + H^+ + e^- + {*}Ru + {*}Pt \quad (5)$$

$$CO_{ads,Pt} + OH_{ads,Ru} \rightarrow CO_2 + H^+ + e^- + {*}Ru + {*}Pt \quad (6)$$

The Pt−Ru assembly on the edge is known to be an active site for the CO oxidation present on Pt phases surrounding the Ru islands.[17,18,23] Recall (Introduction) that two mechanisms account for the promotional effect of Ru: the bifunctional mechanism, where the Ru islands activate water dissociation at lower potentials than Pt (the difference being as high as 300 mV), and the ligand model,[1,3,59,79,80] where ruthenium modifies the electronic structure of the neighboring platinum. More specifically, the formation of a Ru−Pt bond causes a decrease in the Fermi-level local density of states (DOS) on Pt, which in turn reduces the $2\pi^*$ DOS and then the Pt−CO binding energy[3] via the bond order argument. As a consequence, the Ru decoration of a Pt surface leads to a decrease in the CO binding energy on Pt atoms in the close proximity of the Ru islands.[3,81] Samjeske et al. suggested that the first two atomic rows of the Pt sites surrounding the Ru islands are electronically modified by Ru[41] (also, Tong et al.),[81] so that less energy is required to oxidize CO adsorbed on these sites. Subsequently, Lu et al.[82,83] using TPD, and then Wieckowski et al., using ^{13}C EC NMR spectroscopy[3,34,83] demonstrated that the overall CO binding energy modifications play some but relatively minor roles in the enhancement of CO-tolerance, and that the overall activation is mainly due to the bifunctional mechanism.

III.2. Electrochemical Activity for CO Monolayer Electrooxidation. Previous reports established that Ru is indeed promoting the CO oxidation kinetics but concentrated predominantly on optimizing the Ru/Pt composition for the CO-tolerant electrocatalyst.[84,85] New insights in the mechanisms of CO electrooxidation on Pt/Ru surfaces were subsequently obtained by using Ru-decorated Pt surfaces as model electrodes. Thus, in 1993, on the Ru-decorated Pt(110) electrode ($\theta_{Ru} \sim 0.2$), Herrero et al.[22] reported that the stripping voltammetry of methanol chemisorption products (CO-like species) yielded the main electrooxidation peak followed by a shoulder, contrary to what was observed on the homogeneous PtRu alloy surfaces.[8] Subsequently, Friedrich et al.[17] reported that the CO electrooxidation proceeded via an oxidation peak followed by a small shoulder feature on the Ru-decorated Pt(111) electrodes (at $\theta_{Ru} \sim 0.5$). In the same report, two types of CO species of commensurable proportions were found by FTIR,[17] which was confirmed by the recent SFG investigations on Pt(111)/Ru,[57] as well as by Maillard et al.[20] and Park et al.[46] (The latter two on Ru-decorated Pt nanoparticles.) These species are: CO linearly adsorbed on Pt sites and CO linearly adsorbed on Ru sites (see Figure 4). This is in contrast to the FTIR studies on PtRu alloys, where only one CO band was detected,[20,86−88] and confirms that the Ru nanoislands are formed on the Pt surface, as now known from the STM studies.[16,19,23,27,28,32,41,61] Indeed, Zou et al.[88] reported that segregation of Ru into islands with a minimum size of ca. eight atoms is necessary for the CO vibrational feature at the Ru sites to appear as an isolated band in the spectra. Tong et al.[3] confirmed the presence of the two different CO populations on Ru-decorated Pt nanoparticles (see

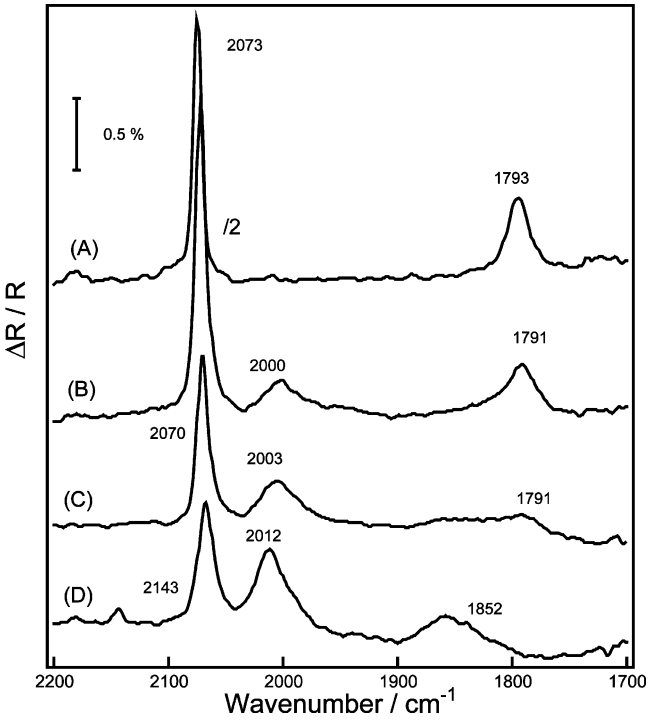

Figure 4. FTIR spectra of adsorbed CO on different Ru-modified Pt(111) electrodes with different Ru coverages. 0.1 M $HClO_4$, $E = 400$ mV vs RHE. (A) Pt(111) without Ru. (B) Pt(111) with $\theta_{Ru} = 0.25$. (C) Pt(111) with $\theta_{Ru} = 0.45$. (D) Pt(111) with $\theta_{Ru} = 0.6$. (Reprinted with permission from ref 19.)

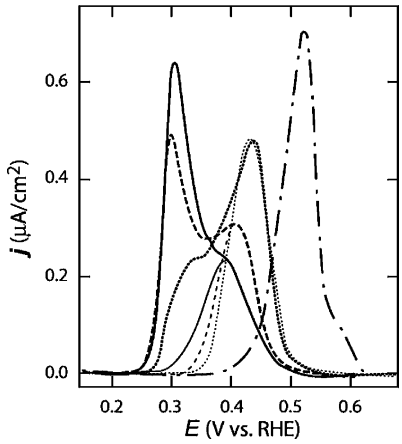

Figure 5. Electrochemical CO stripping voltammograms (10 mV min^{-1}) after 12 h of methanol adsorption at 0.19 V vs RHE for, Pt/Ru-0 (dash−dot), Pt/Ru-14 (dot), −35 (dash), and −53 (solid). These results demonstrate a new, low-potential peak that grows in as the Ru packing density increases. The thin lines represent Gaussian fits to the high-potential peak. (Reprinted from ref 3.)

Figures 5 and 6). In the CO stripping voltammetry, Massong et al.,[42] Davies et al.,[40] and Lu et al.[33,57] (see Figures 7−9) on the Ru-decorated Pt(111) surface; Davies et al.[38,40] on a Ru-decorated Pt(110) electrode; Waszczuk et al.[30] and Maillard et al.[20] on Ru-decorated Pt nanoparticles, reported a pronounced peak splitting contrary to what was observed on the homogeneous PtRu alloys.[8−11]

III.2.1. Influence of the Ru Coverage. It is now well established that the Ru-decorated Pt(111) electrodes studied under voltammetric conditions display a clear CO oxidation peak splitting[33,40] shown in Figures 7 and 10. The data also show a negative ca. 200 mV shift in the CO stripping potential due to the combined effect of the bifunctional and ligand effect, as

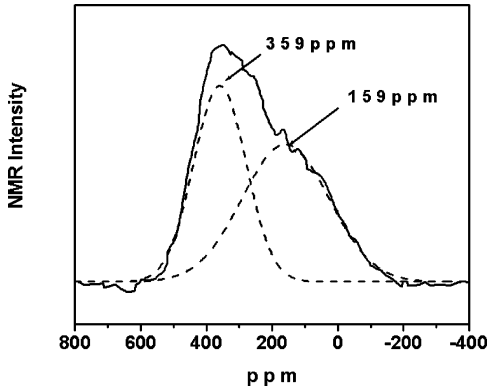

Figure 6. The ^{13}C NMR spectra and double-Gaussian deconvolutions with arrows indicating the spectral positions for ^{13}CO on Pt/Ru-35. (Reprinted from ref 3.)

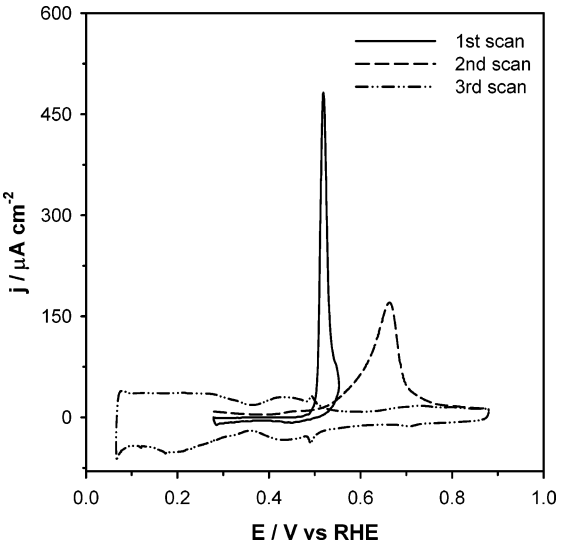

Figure 7. Stripping (50 mV s^{-1}) of a CO adlayer from Pt(111)/Ru (ca. 0.18 ML of Ru) in a CO-free 0.1 M H_2SO_4. First, the potential sweep passed the lower potential voltammetric peak (solid line), and returned to 0.28 V vs RHE. Second, the potential sweep was extended for a complete CO oxidation (dash line). The background scan after CO stripping was also shown (dash−dot−dot line). Exposure of the electrodes to CO at 0.28 V vs RHE for 5 min was followed by Ar purging for 25 min. (Data from Urbana-Champaign.)

discussed above. In terms of the peak morphology, small amounts of ruthenium added to Pt cause the main electrooxidation peak to decrease and broaden, whereas a new oxidation peak on the negative side of the main peak appears. The same effects on the Ru-decorated Pt nanoparticles ($d \sim 3.2$ nm)[3,20]—although less pronounced—were found, and are shown in Figures 5, 11, and 12. (Notice however that different sweep rates are used in these experiments.) CO electrooxidation on Ru-modified Pt−C electrodes ($\theta_{Ru} \sim 0.08$ ML), obtained by spontaneous deposition (see Figure 11), consisted of two overlapping peaks with comparable charges at 0.72 V and 0.81 V vs RHE, respectively. A similar result is observed for $\theta_{Ru}^{LEISS} = 0.04$ ML and $\theta_{Ru}^{XPS} = 0.18$ ML on the Ru-decorated Pt(111) surface (Figure 10). At higher ruthenium coverage, the peak at more positive potential disappears whereas either a single peak or a peak followed by tailing or shoulder is observed. Further increase in the Ru coverage does not lead to more change. The surface Ru-to-Pt atomic ratio to make the most active CO-tolerant electrocatalyst is usually not 50:50 but is of a different value, and this value depends on the type of platinum used as a substrate and the oxidation state of Ru. Note also that the

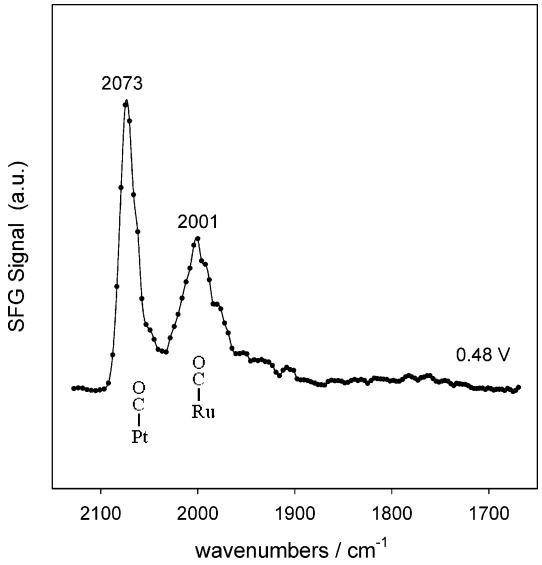

Figure 8. In situ SFG spectrum of chemisorbed CO on Pt(111)/Ru (ca. 0.5 ML of Ru) in a CO-saturated 0.1 M H_2SO_4 solution. (Reprinted with permission from ref 57.)

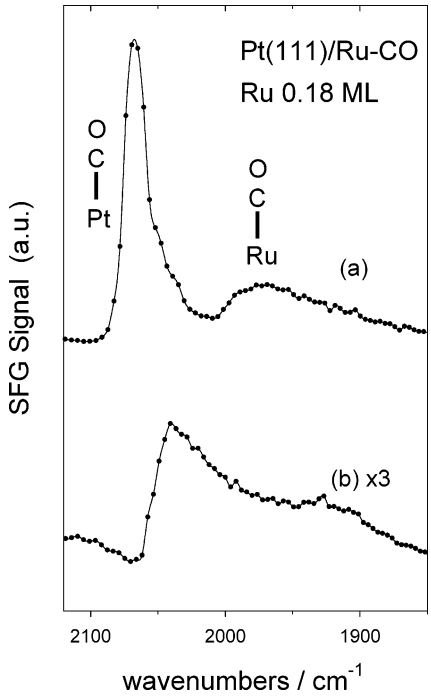

Figure 9. In situ SFG spectrum of chemisorbed CO on Pt(111)/Ru (ca. 0.18 ML of Ru) before (a) and after (b) stripping of Ru−CO in a CO-free 0.1 M H_2SO_4. (Reprinted with permission from ref 57.)

onset of the CO electrooxidation is similar for all Ru-decorated Pt nanoparticles and is Ru coverage dependent,[20] see Table 1.

III.2.2. Influence of Specific Adsorption. It is clear that specific anion adsorption may lead to modifications of the atomic environment of the CO adsorbate and should, in concept, influence the CO_{ads} surface mobility. Indeed, if the adsorbate−adsorbate interaction energies are a few percent of binding energies, they represent a considerably high fraction of the activation energy for diffusion.[89] Davies et al.[40] suggested that the CO mobility could be inhibited by specific adsorption of (bi)sulfate anions in sulfuric acid electrolytes and account for the peak splitting discussed above. However, in perchloric acid, two kinetic regimes were still observed for CO electrooxidation on Ru-decorated Pt nanoparticles[20] as well as on a Ru-decorated Pt(111) surface. Additional understanding of CO electrooxidation mechanisms on the Pt/Ru surfaces, and the role of CO surface mobility in such mechanisms could be obtained by

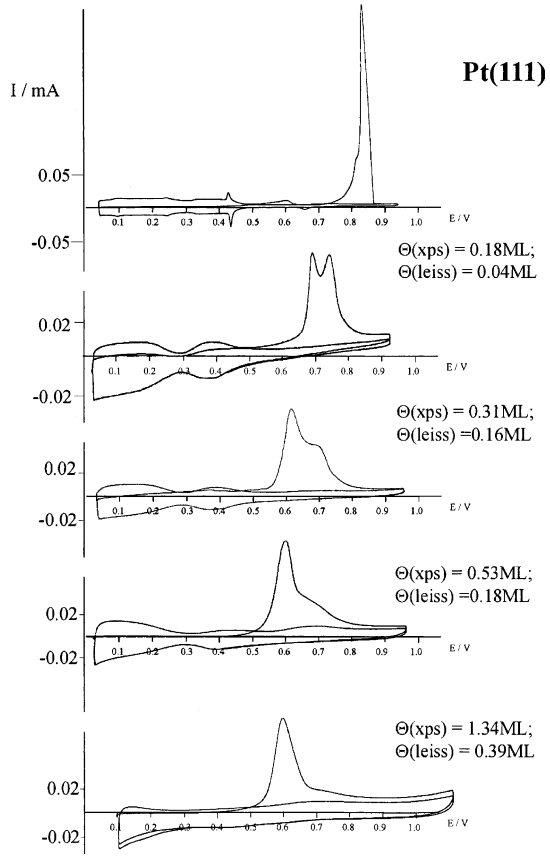

Figure 10. Cyclic voltammetry (0.5 M H_2SO_4, 100 mV s^{-1}) for CO oxidative stripping on clean- and ruthenium-covered Pt(111) surfaces. The ruthenium coverages measured using XPS (θ_{Ru}^{XPS}) and LEISS (θ_{Ru}^{LEISS}) before transfer to the electrochemical cell are indicated. CO was dosed at 0.025 V vs RHE and then oxidatively removed in fresh CO-free electrolyte. (Reprinted with permission from ref 40.)

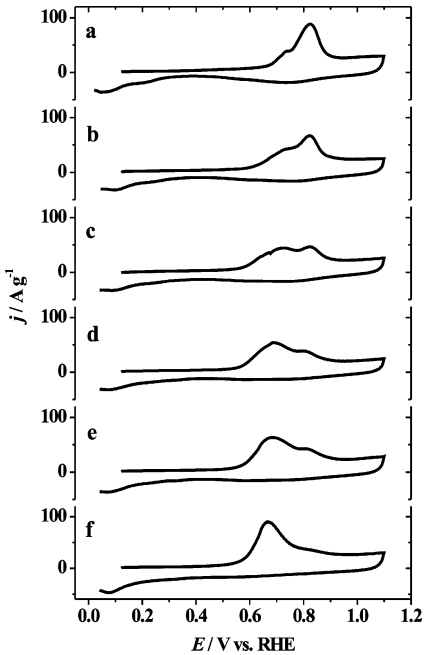

Figure 11. CO stripping voltammetry (20 mV s^{-1}) on a Ru-modified Pt−C electrode by spontaneous deposition in N_2-purged 0.1 M $HClO_4$ with (a) $\theta_{Ru} = 0\%$, (b) $\theta_{Ru} = 3\%$, (c) $\theta_{Ru} = 9\%$, (d) $\theta_{Ru} = 10\%$, (e) $\theta_{Ru} = 14\%$, and (f) $\theta_{Ru} = 22\%$. (Data from Maillard, F., Ph.D., University of Poitiers, 2002.)

TABLE 1: Position of the Atop CO_{ads} Bands (taken at 0.10V vs RHE with a reference spectrum taken at 0.95 V vs RHE) and Onset Potentials for CO Electrooxidation at the Clean and Ru-Modified Pt−C 30% Nanoparticles by Cyclic Voltammetry and "In-situ" Infrared Reflection Spectroscopy

electrode	CO_2 evolution (onset potential)/V	CO oxidation peak potential/V	$\bar{\nu}$ (CO_L/Pt)/cm^{-1}	$\bar{\nu}$ (CO_L/Ru)/cm^{-1}
30% Pt−C	0.65	0.82	2071	
$Ru_{8\%}$/Pt−C[a]	0.45	0.80	2071	2018
		0.73		
$Ru_{10\%}$/Pt−C[b]	0.40	0.80	2071	2017
		0.73		
$Ru_{20\%}$/Pt−C[b]	0.40	0.79	2069	2021
		0.67		
$Ru_{22\%}$/Pt−C[a]	0.40	0.67	2067	2010
$Ru_{36\%}$/Pt−C[b]	0.35	0.67	2064	2021
30% PtRu−C 50:50[c]	0.40	0.62	2052	

[a] Spontaneous deposition. [b] Electrochemical deposition. [c] Electrocatalysts furnished by E-TEK, respectively. (Reprinted with permission from ref 20.)

studies of the CO electrooxidation in different supporting electrolytes, for instance, by systematically going from a nonadsorbing electrolyte ($HClO_4$) to a strongly adsorbing electrolyte (H_3PO_4).

III.2.3. Influence of Chemical Composition and Structure of the Ru Islands on the Electrocatalytic Activity. As underlined in section II.2, Ru adislands of different chemical composition in terms of Ru oxidation state are formed depending on the deposition process. Whereas the Ru adlayers obtained by electrodeposition or under UHV conditions are mainly metallic or can form easily reducible oxides,[29] the spontaneous deposits contain a fraction of Ru oxides and hydroxides that cannot be completely reduced under the previously reported experimental conditions.[26,29,66] Using Pt electrodes modified by spontaneous or electrochemical deposition, Kim et al.[29] demonstrated that metallic ruthenium was a prerequisite for effective methanol electrooxidation, (see also highly relevant work by Viswanathan et al.[90]). Tremiliosi-Filho et al.[26] concluded a similar effect but without providing additional evidence. Maillard et al.[21] confirmed this trend using Pt nanoparticles decorated by Ru spontaneous or electrochemical deposition. Using spontaneous deposition for both Pt(111)/Ru[25] and nanoparticle surfaces,[21] the maximum in electrocatalytic activity toward methanol oxidation at 25 °C was observed at $\theta_{Ru} \sim 20\%$. On the other hand, higher current densities for methanol oxidation were obtained in the case of electrodeposited Ru vs spontaneous deposition.[21] This is consistent with the assumption that the electrocatalytic activity of metallic ruthenium-decorated Pt surfaces (and/or decorated by reducible Ru oxides) is greater than that of Pt surfaces decorated by nonreducible Ru oxides. Concerning CO electrooxidation, Ru-decorated Pt electrodes by spontaneous deposition oxidize CO at a lower overpotential than Ru-decorated Pt electrodes by electrodeposition for similar Ru coverage.[20] Thus, it seems that a sufficient amount of oxygenated Ru species can be formed at lower Ru coverage in the case of spontaneously Ru-modified electrodes to support measurable CO_{ads} oxidation rates. Keeping in mind that the spontaneous deposits contain a fraction of Ru oxides and hydroxides that cannot be reduced, this would imply that a potential region exists where CO and Ru oxides can coexist on the surface. Indeed, Lin et al.[87] observed a current due to OH adsorption before any change in the CO coverage was detected by FTIR. Thus, the peak splitting is independent of the chemical properties of the Ru islands.

Samjeske et al.[41] showed that Ru electrodeposition proceeds mainly on steps on Pt(332), Pt(655), and Pt(755) surfaces. On the other hand, the Urbana and Munich groups have shown homogeneous decoration of the Pt(111) by Ru nanoislands (of ca. 2−5 nm in diameter),[16,18,23,28,32] i.e., no preferential deposition sites. In both cases, if the Ru coverage is properly monitored between 0 and 0.2 ML, a peak splitting is observed and the resolution of this split is relatively high. Thus, the possibility of the peak splitting to arise from the "site blocking process" of electrodeposited Ru should be discarded. Notably, if the latter were true, the Ru electrodeposited at steps or on terraces would work differently for the promotion of CO electrooxidation. However, in contrast to the above, Hayden et al. performed experiments that clearly demonstrated that the peak splitting was influenced by the type of the Ru disposition at the Pt surface. In the quoted study, the Pt(111) and Pt(533) (four terrace atoms of Pt(111) and (100) steps) surfaces[91] were decorated by Ru using spontaneous deposition or spontaneous deposition followed by a reduction in a 10% H_2 in Ar atmosphere. For Pt(111)/Ru, a decrease in both the onset and the peak potential of CO electrooxidation was found, in contrast to that for Pt(533)/Ru, suggesting that the (100) steps provide enough nucleation centers for the OH formation to be used for the CO removal from the surface. However, when the Pt(533)/Ru surface was reduced in the hydrogen atmosphere, a peak splitting reappeared. This was interpreted under the assumption that the metallic ruthenium was decorating the inside step edges of Pt(533), forming linear arrays of PtRu ensembles, highly active for CO electrooxidation.

Notice, however, that another possibility to account for the data discussed above is that the Ru islands have different local density of states and different electrocatalytic activities when deposited on steps than on terraces. Indeed, according to the density functional calculations performed by Hammer et al.,[92] CO chemisorption energy increases from ~1.25 eV for a Pt(11 8 5) terrace site to 1.45 eV for a (111) terrace site, 1.55 eV for a (100) terrace site, 1.95 eV for a (11 8 5) step site and 2.15 eV for a (11 8 5) kink site. The same idea may be applied to Ru islands deposited on Pt nanoparticles that can behave differently than Ru deposited on Pt(*hkl*) surfaces. More work is needed to amplify these new concepts in the field of Pt/Ru CO oxidation electrocatalysis.

III.2.4. Toward Understanding of the Origin for the Peak Splitting in CO Stripping Voltammetry. As already reviewed above, two different CO populations have been resolved on the Ru-decorated Pt surfaces by FTIR, EC NMR, and SFG spectroscopies[3,16−20,31,46,57] as well as by CO stripping voltammetry.[20,30,33,40,42,50,55] On the Ru-decorated Pt surfaces at low Ru coverage (at $\theta_{Ru} < 0.2$ ML), a peak splitting was found in the CO stripping voltammetry. It is known that CO can adsorb on a bulk ruthenium electrode[4,11,13] and is then voltammetrically oxidized, yielding a broad CV peak located around 0.6 V vs

RHE. Thus, on the Ru-decorated Pt surfaces discussed above, the more negative peak can be assigned to the CO oxidation on the Ru islands on Pt. Similarly, since the charge under this peak is too large to correspond to CO oxidation on the Ru islands alone, one may conclude that the charge also originates from the CO present on Pt sites adjacent to the Ru islands (Pt−Ru edge). Then, the active site for the CO electrooxidation is defined as the Pt−Ru edge plus the Pt atoms surrounding Ru islands (see section III.1). This is, in our view, a new formulation of the Watanabe and Motoo bifunctional mechanism[4] now applied to heterogeneous, Ru-island decorated surfaces.

We demonstrated above a pronounced influence of the chemical and structural properties of the Ru islands on reduction in the overpotential for the CO electrooxidation on Pt/Ru surface, and on the voltammetric CO oxidation peak splitting, or the absence of it. However, a shoulder or a tailing in the CO stripping voltammetry is quite persistent even at high Ru coverage, and this may be interpreted as due to the CO (or OH_{ads}) surface diffusion limitation of the reaction rate, or a slow reaction rate at the Pt/Ru edge. According to Monte Carlo simulations for the CO stripping voltammetry,[58,93] the slow CO mobility from Pt to Ru sites should lead to a "two peaks" voltammetric CO stripping behavior. On the other hand, Davies et al. suggested a slow OH_{ads} diffusion or (bi)sulfate adsorption[40] to be the origin of the peak splitting. The Wieckowski group proposed, however, the CO oxidation kinetics to be predominantly limited by a slow oxidation reaction at the Pt/Ru edge.[3,33]

IV. Models Accounting for the CO Stripping Voltammetry on the Pt/Ru Surfaces

IV.1. Definition and the Validity of the Models. Based upon literature data summarized above, several models for the CO oxidation on Pt/Ru surfaces can be distinguished. In all models, CO species are assumed adsorbed at Ru and Pt sites and at the Pt sites in close proximity of the Ru sites. What is also common to all the models is that the oxidation of the CO species adsorbed at Pt sites not adjacent to the Ru sites occurs at a lower potential than for pure Pt surfaces.[3,79] The models then can be depicted as follows:

1st Model. There is no CO mobility on the surface (the CO molecules are rigid), and CO on Ru and CO on Pt sites are isolated populations, leading to a first peak of CO oxidation on Ru and in the vicinity of Ru islands, and a second peak due to the CO oxidation on Pt.

2nd Model. It assumes fast CO diffusion rate and fast reaction kinetics leading to a single peak for all Ru coverages.

3rd Model. One then assumes that the CO diffusion rate is high but finite[16−19,58,93] and that the CO oxidation at the Pt sites in the close proximity of the Ru island edge takes place at, or very near, the potential for the CO oxidation on Ru. The key parameter for the reactivity then is the distance between the two closest Ru islands separated by a few or several interatomic Pt−Pt distances. If this distance is sufficiently large, the reactivity is influenced by the CO surface diffusion, either from the bare Pt sites to the Ru sites at the Pt/Ru edge[17,18] or from the bare Pt sites to the Pt sites directly at the edge of the Ru islands, which are electronically modified by the neighboring Ru present.[58,93] That is, this model assumes the diffusional limitation of the CO reactivity on the Pt/Ru surfaces.

4th Model. Within the realm of this model, the CO mobility on Pt is infinitely fast, so that the CO is always available for reaction at the Pt/Ru edge. At the same time, the Pt sites close to the Ru islands are covered by OH_{ads} but the reaction of CO with the OH_{ads} is relatively slow, which limits the kinetics of CO electrooxidation.[3,33] This also gives rise to two CO peaks in cyclic voltammetry, the first on top of the Ru islands and the second, more positive, at the Pt/Ru edge. This model assumes the reaction limitation of the CO reactivity on the Pt/Ru surfaces.

5th Model. This model is based upon the hypothesis that the oxidant species (OH_{ads}, O_{ads}) may diffuse from the Ru islands to bare Pt sites, and refers to OH spillover on fuel cell catalysts reported in the subject literature.[40]

On single-crystal platinum surfaces, the Koper group invalidated model #1 by showing that the CO oxidation on the stepped Pt surfaces occurs via a single peak.[94] The data can be taken in favor of fast CO diffusion on smooth Pt electrodes, and data by Lu et al. on Pt(111)/Ru are quite suggestive toward this end.[33] On 6−10 nm Pt nanoparticles, EC NMR diffusion data show that the CO motions are also fast, and they give essentially the same activation energy for surface diffusion as observed in gas phase (or UHV). Slow (but finite) CO diffusion was considered on smaller Pt nanoparticles, and it was concluded[95] that the smaller the particles, the lower the CO diffusion coefficient. Overall, however, the assumption of a rigid CO network on platinum or Pt/Ru cannot be sustained.

We believe that model #2 is also incorrect as it gives only one CO stripping peak for all Ru coverages, in contrast to the results of the experiments of Massong et al., Davies et al.,[38−40] and Lu et al.[33,57] on the modified Pt(*hkl*)/Ru surfaces, and by Waszczuk et al.[30] and Maillard et al.[20] on the Ru-decorated Pt nanoparticles. For model #3, the slow diffusion between Ru and Pt sites results in a "two peak" behavior for the CO electrooxidation at low Ru coverages, $\theta_{Ru} < 20\%$.[20,40] Increasing the Ru coverage maximizes the number of Pt−Ru active sites, increases the long-range electronic effect of Ru on Pt atoms, and results in disappearance of the peak associated with the CO electrooxidation at the "bare" Pt surface. A shoulder or a tailing are then expected in the CO stripping voltammetric or chronoamperometric measurements, respectively. The third model therefore fits the experimental data very well.

In model #4, the origin of the peak splitting is due to the slow reaction between CO molecules adsorbed on Pt sites but at close distance to the Pt/Ru edge.[33,57] Apparently, this is also a good model to account for the CO stripping data discussed in this review.

Finally, model #5 appears to be very unlikely because of an unfavorable thermodynamic barrier (Ru binds OH stronger than Pt does), and quantum-chemical data indicate that the OH_{ads} binding energy does not increase on Pt modified by Ru.[58] Therefore, with respect to the discrimination between the diffusion-controlled and reaction-controlled processes, only models 3 and 4 should further be considered, and the CO_{ads} surface mobility (diffusion) may be the essential factor in the kinetics of CO electrooxidation on Ru-decorated Pt surfaces. Below, we will briefly discuss the methods and experimental conditions used in the literature to quantify the CO_{ads} surface diffusion, a possible effect of the Pt substrate on CO_{ads} diffusion, and we will use relevant examples from literature as a tool to distinguish between models 3 and 4.

IV.2. Diffusion vs Reaction Limited Process. *IV.2.1. CO Surface Diffusion, the Substrate Effect.* It is well-known from heterogeneous gas-phase catalysis[89,96] that under constant coverage conditions, surface mobility of an adsorbate is caused by its random, thermal mobility. This is a Brownian motion occurring at equilibrium and in the absence of external forces. An adsorbed particle is then able to move from a binding site, where it has the lowest energy, to another equivalent binding site without very much expenditure of energy, and without any memory of its motions on the surface (uncorrelated jumps). However, the distribution of the binding sites depends on the

morphology of the surface on which the adsorbate resides. If the adsorbate is CO and the surface is platinum, the CO diffusion coefficient, D_{CO}, may differ significantly, depending on the Pt surface and on the Ru addition to the surface. If a large difference in the CO binding energy exists on the Pt surface, then the CO_{ads} mobility can be significantly slowed. This is the case, for example, of a Pt-stepped surface where an additional barrier (the Schwoebel−Ehrlich barrier)[97] is present at the upper edge, whereas an additional trapping potential is present at the lower step edge. Thus, the steps or defect sites, which are known to adsorb CO preferentially, may act as surface traps.[98] Recently, Koper et al.[93] fitted CO electrooxidation transients on different stepped surfaces, presenting different step densities, with a mean field model approximation (where diffusion rates are supposed to be much faster than reaction rates). The absence of tailing in the chronoamperometric experiments (which is usually suggesting restricted CO_{ads} mobility) was consistent with the fact that steps act as active sites for water dissociation and further dissociation to yield the oxygen-containing species. Interestingly, the only stepped surface showing some tailing after the current maximum was the Pt(553) surface, i.e., the surface presenting the highest step density. The authors suggested this tailing to be the result of slow oxidation of CO adsorbed on steps.

On Pt nanoparticles, a decrease of D_{CO} is expected due to the large fraction of edges and corner sites, both of which increase in prevalence with a decrease in the particle size. Indeed, Bercerra et al.[99] using ^{13}C surface NMR to investigate the mobility of CO_{ads} on alumina-supported Pt clusters found a considerable increase in the activation energy for CO_{ads} diffusion (E_{diff}) with a decrease of the Pt particle size. Maillard et al.[95] performed CO electrooxidation transients on Pt nanoparticles of different sizes. A long tailing was observed after the current maximum, which is more pronounced the smaller the particle size is. This suggests restricted CO_{ads} mobility at Pt nanoparticles below ca. 2 nm size, with the diffusion coefficient strongly dependent on the particle size. Thus, although a similar peak splitting has been reported in the CO stripping voltammetry on Ru-decorated Pt nanoparticles or Pt(*hkl*) surfaces, it's origin may be different because of a pronounced substrate effect. Similarly, the crystallographic orientation of the Pt substrate may influence the CO_{ads} surface mobility because distinct energy barriers exist for hopping along the (111), (100), or (110) surfaces. Depending on the terrace orientation, different CO diffusion coefficients are therefore expected, which may influence the CO electrooxidation kinetics. However, the modifications of D_{CO} will not be large enough to induce a transition between the diffusion-controlled and reaction-controlled kinetics.

In summary, the literature survey also suggests that CO mobility on Ru-decorated Pt surfaces should be regarded as an important parameter in the kinetics of reaction. Depending on the type of Pt surface, the value of D_{CO} may control the transition between reaction and diffusion-limited regimes.

IV.2.2. Restricted CO Mobility on Ru-Decorated Pt Surfaces? Koper et al. reported recently 10^{-11} cm^2 s^{-1} as a lower limit for the CO_{ads} diffusion on Pt(111) and stepped Pt[n(111) × (111)] surfaces.[93] However, both experimental data as well as model simulations suggest a restricted CO_{ads} mobility on bimetallic Pt/Ru surfaces. D_{CO} on Ru-modified Pt(111) was estimated by Friedrich et al.[19] as $\geq 4 \times 10^{-14}$ cm^2 s^{-1}, and $\leq 3 \times 10^{-17}$ cm^2 s^{-1} by Samjeske et al.[41] A likely reason for the 3 orders of magnitude change of D_{CO} was indicated by Samjeske et al.[41] who assumed a weaker CO binding to a Pt atom, which has Ru neighbors than to the "bare" Pt, in agreement with Buatier de Mongeot et al.[80] This makes the overall diffusion from bare Pt to the Pt sites in the close proximity of Ru islands a very slow process (the "uphill diffusion") and the diffusion of CO_{ads} from Pt sites in close proximity of Ru islands to these Ru islands a fast process. In FTIR, the band attributed to the linear CO on Pt is red-shifted upon increasing coverage of Ru obtained either by electrochemical or spontaneous deposition.[19,20,46] This shift in the CO stretching wavenumber reflects a different electron density at the CO molecule when Ru is added. In terms of the metal−CO bond strength however, FTIR experiments are not very informative as there is no apparent correlation between the binding energy of CO and the internal C−O stretching frequency.[100] This issue therefore should be further investigated.

IV.2.3. Diffusion vs Reaction Limited Process. To check if the two CO populations (see above) can be electrochemically separated, Massong et al.[42] performed electrooxidation of adsorbed CO at a constant potential on Ru-decorated Pt(332) and Pt(111) surfaces. After a potential step to 0.44 V vs RHE for 2 min, approximately 70% of the adsorbate was oxidized, but a small oxidation current was still visible. At higher potentials, a higher portion of the CO monolayer was oxidized in the same 2 min of the experiment. This agrees very well with both models 3 and 4. Namely, the small, nearly constant CO_2 formation rate may indicate a slow oxidation process determined either by the slow CO_{ads} diffusion, or by the slow oxidation at the PtRu edge. However, if the CO diffusion was a slow process,[19,20,47] the CO molecules could effectively repopulate the Pt sites in the close proximity to Ru islands under both potentiostatic[19,20] and ocp conditions.[47] Indeed, during a potentiostatic step at 0.45V vs RHE, i.e., at a potential where water does not yet dissociate on Pt, the FTIR band intensities corresponding to the linear CO adsorbed on Ru and Pt decrease simultaneously on a time scale of minutes due to the CO electrooxidation process.[19,20] On the other hand, Park et al.[46] on nanoparticle surface and Lu et al. on Pt(111)/Ru[57] reported that the band corresponding to the CO adsorbed on Ru sites disappears first, which is only then followed by disappearance of the band corresponding to CO adsorbed on the Pt sites. This could be an indication that the two CO populations behave independently, both in the electrochemical and spectroscopic experiment, and that the first electrooxidation of CO occurs on Ru sites and then on Pt sites. Note however that the band corresponding to CO adsorbed on Ru sites "survives" up to 0.2 V vs Ag/AgCl in the case of Park et al., which is the potential at which the potentiostatic measurements of Maillard et al. have been performed.[20] So, these two experiments are not contradictory. Note also different experimental conditions used in the reported investigations. Indeed, to reduce the CO dipole−dipole coupling between Pt and Ru regions in the nanoparticle study of Park et al.[46] which affects both bandwidths and intensities (intensity transfer from the lower to the higher wavenumbers), only low CO coverage (0.3 ML) was used in contrast to a CO saturation coverage in the case of Maillard et al.[20] Moreover, the repeated spontaneous deposition that was used by Crown et al. to create the Pt/Ru surfaces leads to multilayer Ru island formation on Pt(*hkl*) surfaces.[32] For instance, when used to add Ru to the Pt(111) surface, the island height was found to be up to 1.0 nm (that is, 4 ∼ 5 layers). In contrast, Friedrich et al.[19] used electrochemical deposition that created monatomic Ru islands, at least at Ru coverage below 0.4 ML (the terms "coverage" and "packing density"[30] are then equivalent). It appears therefore to be difficult to compare the experiments performed on different Pt substrates (the nanoparticle Pt black in the case of Park, and the Pt(111) electrode as substrates in the case of Friedrich), with different Ru coverages. Moreover, the influence of the size as well as the height of Ru−Ru ensembles should carefully be investigated since it is obvious that monatomic Ru islands are electronically modified by the

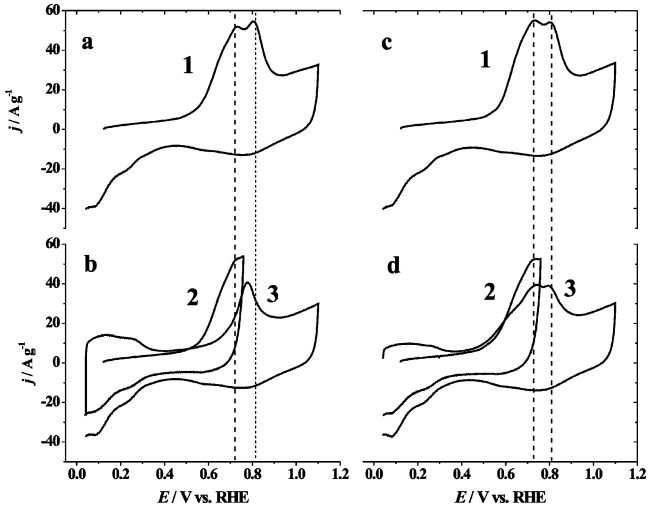

Figure 12. CO stripping voltammetry (20 mV s^{-1}) on a Ru-modified Pt−C electrode in N_2-purged 0.1 M $HClO_4$. Ru electrochemical deposition: $\theta_{Ru} \approx 8\%$. (a, c) (1) First cycle between 0.1 and 1.1 V vs RHE. (b, d) (2) Second cycle between 0.1 V → 0.76 V → 0.1 V vs RHE (3) Third cycle between 0.1 and 1.1 V vs RHE. (Reprinted with permission from ref 20.)

underlying Pt substrate, whereas the multilayer height Ru islands are expected to have properties closer bulk Ru electrodes.

Maillard et al.[20] carried out a simple experiment to prove that CO can repopulate Pt atoms in the close proximity of Ru islands but, at the same time, the CO surface mobility is a slow process (cf. Figure 12). The authors used an electrode composed of Ru-decorated Pt nanoparticles ($\theta_{Ru} = 0.08$ ML) and performed CO stripping between 0.1 and 1.1 V vs RHE (cf. Figure 12, cycle (1)). They confirmed that the cyclic voltammetry exhibits two CO stripping peaks at 0.73 and 0.80 V vs RHE attributed to the CO adsorbed on and near Ru islands and the CO on the Pt phases, respectively. (The separation between the two peaks displays a saddle point at $E \sim 0.76$ V.) A CO monolayer was next readsorbed to the Pt/Ru electrode, the solution was purged and then, a potential program: 0.1 V → 0.76 V → 0.1 V at the same sweep rate was applied. The third cycle from 0.1 V → 1.1 V vs RHE was recorded to test if CO had moved from Pt sites to Ru and Pt near Ru island sites. The second cycle presents a peak at $E \sim 0.73$ V vs RHE, and a single peak at $E \sim 0.78$ V vs RHE was observed in the third cycle (part b of Figure 12, cycles 2 and 3). In Figure 12, it is obvious that (1) ∼ (2) + (3) and that no exchange seems to occur, as concluded previously.[3,101] However, if a similar potential program with a potential step at 0.1 V vs RHE over a period of 1800 s between cycle (2) and (3) was performed (part d of Figure 12), this yields two peaks of equal charges in the cycle (3) at $E \sim 0.73$ and 0.80 V vs RHE. This experiment voltammetrically confirms that CO_{ads} surface mobility across the Pt/Ru edge leading to CO electrooxidation is a very slow but a finite process.

Friedrich et al. also performed some transients for CO monolayer electrooxidation at 0.45, 0.5, and 0.6 V vs RHE in 0.1 M $HClO_4$[19] (see Figure 13). This figure shows clearly a tailing current after the current maximum at each investigated potential, which fits the kinetic model of an active site, Pt−Ru edges, and restricted CO mobility. In the case of high CO mobility, the shape of the potentiostatic CO oxidation transients would have been symmetric, resembling transients observed on Pt(111), which can be predicted by the mean-field approximation.[94] Lu et al.[33] used a double-potential step chronoamperometry from 0.25 to 0.52 V for 2 s followed by a second potential step to 0.67 V vs RHE in order to investigate the

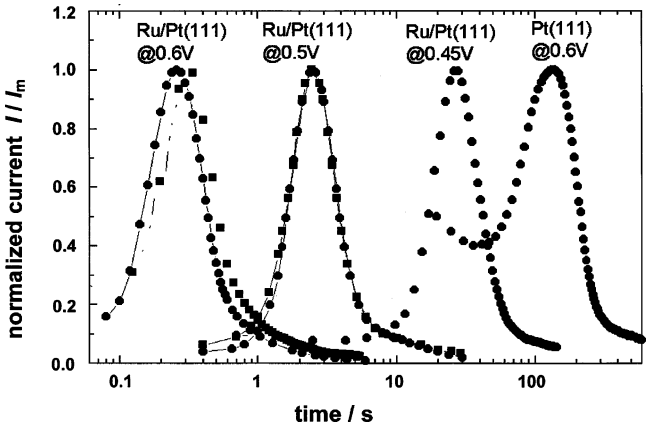

Figure 13. Current transients of potentiostatic CO monolayer oxidation in 0.1 M $HClO_4$ for Pt(111)/Ru ($\Gamma_{Ru} = 0.25$) and Pt(111) at oxidation potentials of $0.45 \leq E_{ox} \leq 0.6$ V vs RHE. For Pt(111)/Ru at $E = 0.6$ and 0.5 V vs RHE, data from two different electrodes but obtained under the same preparation conditions are superimposed in order to indicate the reproducibility. (Reprinted with permission from ref 19.)

mechanisms of reaction on Ru-decorated Pt surface. The electrooxidation of CO population corresponding to the lowest peak potential occurs through a symmetric current−time peak response, typical of a Langmuir−Hinshelwood mechanism. This shows that the oxidation process is activated uniformly across a Ru island without any diffusion process necessary. A current decay rather than an oxidation peak, followed by a current−time tailing, was observed in the second potential step. This was interpreted as (i) the change of mechanism from a Langmuir−Hinshelwood to a first-order kinetics (see above) or (ii) a diffusional limitation as discussed previously. In such a case, the difference with the Koper data is that the Pt atoms surrounding the Ru islands are expected to be the active sites for CO electrooxidation.

Tong et al. have reported the split peak behavior for CO electrooxidation (coming from methanol dehydrogenation) at 10 mV min^{-1} (∼15 min between the two peaks) with a Ru coverage of $\theta_{Ru} = 0.53$ obtained by repeated spontaneous deposition[3] (Figure 5). They concluded that for a low sweep rate and high Ru coverage, the reaction between Ru−OH and Pt−CO is the rate-determining step because there is no limitation by diffusion (every Pt atom is in close proximity of Ru islands). Thus, regarding the hypothesis of model 3, a single peak is expected in the cyclic voltammetry. In the case of the reaction limitation at the Pt−Ru edge, the peak splitting is expected, which is the case in this quote study. One may, however, argue that under such Ru coverage conditions, every Pt atom should be in close proximity of Ru islands and be "electronically modified" by the surrounding Ru atoms. However notice that the effective Ru coverage is not θ_{Ru} but less than 0.53 (the latter value corresponds to the packing density, see above) due to the 3D growth of the Ru islands after a multiple spontaneous deposition.[23,32] Indeed, on Pt(111), it has been shown that after four depositions, approximately 30−35% of the Pt surface is covered with ruthenium islands of varying heights. About 65% of the islands are a monolayer high, while 25% consists of two ruthenium layers and 10% consists of three monolayers or higher. Thus, if the true coverage of Ru at 0.53 should indeed yield a tailing (or a shoulder type) rather than a split behavior, as a major part of the CO molecules are already forced to be in an adjacent position to Ru−OH, and the CO molecules would only have to hop to this adjacent position. This would then cause the shoulder to be observed. Another possibility to account for the data however may arise from the intrinsic nature of the nanoparticles used. Indeed, a nanoparticle is composed of

different adsorption sites (the high coordinated terraces and low coordinated edges). Since the low coordination sites are known as oxygen species nucleation centers,[41,52] one would expect CO stripping from Pt nanoparticles to occur at the lower overvoltage than from Pt(111). However, when comparing the peak position of the CO stripping peak from the nanoparticle and single crystalline surfaces, it is seen that the oxidation of the whole CO monolayer requires much higher overpotential on the nanoparticles than on any of the extended surfaces so far explored.[95,102] Such a high overvoltage can be related to the high proportion of edges and vertices sites, which bind CO stronger than terraces and can even trap the CO for a considerable time.[102] Within model 4, the reaction at the Pt−Ru edge may become rate limiting because the rds changes from an electron transfer from the reactant pair CO and OH (Pt−O−H···O≡C−Pt) on the terraces to a chemical step when the Pt terraces are modulated by the edges. Then,[33] the reaction between Pt−OH present around the Ru islands and the CO adsorbed on the bare Pt atoms is the dominating process.

V. Conclusions

We have reviewed CO oxidation electrocatalysis on Pt electrodes decorated by ruthenium as a model electrochemical reaction on bimetallic surfaces. Various Pt/Ru formulations were used to shed light on the mechanism and kinetics of the electrooxidation process. It appears that two types of CO species have been identified: the linear CO adsorbed on Ru sites and the linear CO adsorbed on Pt sites. These two CO species can be consecutively electrooxidized on the positive-going voltammetric scan to give rise to the characteristic peak splitting in the stripping reaction. The peak split exposes a slow CO oxidation kinetics at the Ru sites that are, as reviewed above, present as Ru islands on the Pt substrate. The split is removed with the increase in the Ru coverage. While the CO appears strongly bound to the Ru and Pt sites, recent measurements indicate that the exchange between the CO populations on the Ru and Pt sites is possible, proving that the CO may move over the Pt/Ru edge at a certain rate. Further, the Pt−Ru edge was identified as providing the active sites for water dissociation needed to generate OH species to react with CO. Soon after the CO oxidation begins (or during a steady-state methanol oxidation), the Pt sites surrounding the Pt/Ru edge are covered by hydroxy groups that coexist with CO on the Pt surface. The CO oxidation reaction then involves a reactant pair (Pt−O−H···O≡C−Pt) that decomposes yielding CO_2 and solution protons; the process is strongly electrode potential dependent.[33] The issue how the CO can get to the Pt/Ru edge was addressed by Friedrich et al.[19] who assumed CO_{ads} surface diffusion from the bare Pt to the Ru islands. In expansion of this surface mobility concept, a local CO surface transport limitation (near the edge) via the uphill diffusion from Pt sites to neighboring Pt/Ru edge sites[41] was postulated to account for the peak splitting behavior. Another possibility to explain the split and the related slow CO oxidation kinetics at the edge is a slow change in the oxidation state of Ru, which in turn induces a slow delivery of OH for the reaction. At present, however, it is difficult to distinguish whether the reaction is limited by such oxidation kinetics at the Pt/Ru edge or by the CO diffusion to the Pt/Ru edge.

In the perspective of this reviewed research, the challenge for electrocatalysis is to increase the catalytic activity and stability of electrochemical materials well beyond the Pt/Ru catalysis level to support robust fuel cell performance for a variety of applications. Judging from the current status of the field, the challenge will be met by further progress in experimental and theoretical tools of electrochemical surface science and electrocatalysis. As indicated in this report, many surface analytical techniques can now be brought to bear to arrive at realistic views of electrochemical reactions having the direct connection to fuel cell catalysis domains. Still, introduction of new techniques will be welcome to accelerate the rate of new discoveries. We notice that most of the studies available to date have predominantly examined bimetallic systems, either substrate/admetal or alloys. Future studies will systematically focus on ternary and higher order systems examining new atomic ensembles and surface structure. Metal/substrate interactions will further be investigated on the electronic level, including noble metal/semiconductor catalytic interfaces. Finally, improving the theoretical tools beyond the current DFT level, especially for computational syntheses of new catalytic materials,[103] is a precondition for more realistic applications of theory to electrocatalytic systems.

Acknowledgment. This work is supported by the U.S. Department of Energy, Division of Materials Sciences under Award No. DEFG02-91ER45439, through the Frederick Seitz Materials Research Laboratory at the University of Illinois at Urbana-Champaign, and by the National Science Foundation under grant NSF CHE03-4999. Additional support was provided by the Army Research Office (A.W.). Financial support by the Deutsche Forschung Gemeinschaft (DFG) under contracts Sti74/8-4 and 436RUS113-718-1-1 and by HGF/BMBF/NRC (Contract No. 01SF 0201) is gratefully acknowledged (U.S.). We also want to thank Dr. Elena Savinova and Dr. Antoine Bonnefont for fruitful discussions.

References and Notes

(1) Krausa, M.; Vielstich, W. *J. Electroanal. Chem.* **1994**, *379*, 307.
(2) Frelink, T.; Visscher, W.; Vanveen, J. A. R. *Surf. Sci.* **1995**, *335*, 353−360.
(3) Tong, Y. Y.; Kim, H. S.; Babu, P. K.; Waszczuk, P.; Wieckowski, A.; Oldfield, E. *J. Am. Chem. Soc.* **2002**, *124*, 468.
(4) Watanabe, M.; Motoo, S. *J. Electroanal. Chem.* **1975**, *60*, 267.
(5) Yajima, T.; Wakabayashi, N.; Uchida, H.; Watanabe, M. *Chem. Commun.* **2003**, 828−829.
(6) Petrii, O. A. *Dokl. Akad. Nauk SSR* **1965**, *160*, 871.
(7) Binder, H., Kohling, A., Sandstede, G., Barker, B. S., Eds.; Academic Press: New York-London, 1965; p 91.
(8) Gasteiger, H. A.; Markovic, N.; Ross, P. N.; Cairns, E. J. *Electrochim. Acta* **1994**, *39*, 1825.
(9) Aberdam, D.; Durand, R.; Faure, R.; Gloaguen, F.; Hazemann, J. L.; Herrero, E.; Kabbabi, A.; Ulrich, O. *J. Electroanal. Chem.* **1995**, *398*, 43.
(10) Gasteiger, H. A.; Markovic, N. M.; Ross, P. N. *J. Phys. Chem.* **1995**, *99*, 16757.
(11) Kabbabi, A.; Faure, R.; Durand, R.; Beden, B.; Hahn, F.; Leger, J. M.; Lamy, C. *J. Electroanal. Chem.* **1998**, *444*, 41.
(12) Schmidt, T. J.; Gasteiger, H. A.; Behm, R. J. *Electrochem. Commun.* **1999**, *1*, 1.
(13) Lin, W. F.; Zei, M. S.; Eiswirth, M.; Ertl, G.; Iwasita, T.; Vielstich, W. *J. Phys. Chem. B* **1999**, *103*, 6968.
(14) Hoster, H.; Iwasita, T.; Baumgartner, H.; Vielstich, W. *J. Electrochem. Soc.* **2001**, *148*, A496.
(15) Janssen, M. M. P.; Moolhuysen, J. *Electrochim. Acta* **1976**, *21*, 861.
(16) Cramm, S.; Fiedrich, K. A.; Geyzers, K. P.; Stimming, U.; Vogel, R. *Fresen. J. Anal. Chem.* **1997**, *358*, 189.
(17) Friedrich, K. A.; Geyzers, K. P.; Linke, U.; Stimming, U.; Stumper, J. *J. Electroanal. Chem.* **1996**, *402*, 123.
(18) Friedrich, K. A.; Geyzers, K. P.; Marmann, A.; Stimming, U.; Vogel, R. *Z. Phys. Chem.* **1999**, *208*, 137.
(19) Friedrich, K. A.; Geyzers, K. P.; Dickinson, A. J.; Stimming, U. *J. Electroanal. Chem.* **2002**, *524*, 261.
(20) Maillard, F.; Gloaguen, F.; Hahn, F.; Leger, J.-M. *Fuel Cells* **2002**, *2*, 143.
(21) Maillard, F.; Gloaguen, F.; Leger, J. M. *J. Appl. Electrochem.* **2003**, *33*, 1.
(22) Herrero, E.; Franaszczuk, K.; Wieckowski, A. *J. Electroanal. Chem.* **1993**, *361*, 269.

(23) Herrero, E.; Feliu, J. M.; Wieckowski, A. *Langmuir* **1999**, *15*, 4944.
(24) Chrzanowski, W.; Wieckowski, A. *Langmuir* **1997**, *13*, 5974.
(25) Chrzanowski, W.; Wieckowski, A. *Catal. Lett.* **1998**, *50*, 69.
(26) Tremiliosi, G.; Kim, H.; Chrzanowski, W.; Wieckowski, A.; Grzybowska, B.; Kulesza *J. Electroanal. Chem.* **1999**, *467*, 143−156.
(27) Crown, A.; Wieckowski, A. *Phys. Chem. Chem. Phys.* **2001**, *3*, 3290.
(28) Crown, A.; de Moraes, I. R.; Wieckowski, A. *J. Electroanal. Chem.* **2001**, *500*, 333.
(29) Kim, H.; de Moraes, I. R.; Tremiliosi, G.; Haasch, R.; Wieckowski, A. *Surf. Sci.* **2001**, *474*, L203.
(30) Waszczuk, P.; Solla-Gullon, J.; Kim, H. S.; Tong, Y. Y.; Montiel, V.; Aldaz, A.; Wieckowski, A. *J. Catal.* **2001**, *203*, 1.
(31) Babu, P. K.; Tong, Y. Y.; Kim, H. S.; Wieckowski, A. *J. Electroanal. Chem.* **2002**, *524*, 157.
(32) Crown, A.; Johnston, C. M.; Wieckowski, A. *Surf. Sci.* **2002**, *506*, L268.
(33) Lu, G.-Q.; Waszczuk, P.; Wieckowski, A. *J. Electroanal. Chem.* **2002**, *532*, 49.
(34) Waszczuk, P.; Lu, G. Q.; Wieckowski, A.; Lu, C.; Rice, C.; Masel, R. I. *Electrochim. Acta* **2002**, *47*, 3637.
(35) Vigier, F.; Gloaguen, F.; Leger, J. M.; Lamy, C. *Electrochim. Acta* **2001**, *46*, 4331.
(36) Jarvi, T. D.; Madden, T. H.; Stuve, E. M. *Electrochem. Solid State Lett.* **1999**, *2*, 224.
(37) Iwasita, T.; Hoster, H.; John-Anacker, A.; Lin, W. F.; Vielstich, W. *Langmuir* **2000**, *16*, 522.
(38) Davies, J. C.; Hayden, B. E.; Pegg, D. J. *Electrochim. Acta* **1998**, *44*, 1181.
(39) Davies, J. C.; Hayden, B. E.; Pegg, D. J. *Surf. Sci.* **2000**, *467*, 118.
(40) Davies, J. C.; Hayden, B. E.; Pegg, D. J.; Rendall, M. E. *Surf. Sci.* **2002**, *496*, 110.
(41) Samjeske, G.; Xiao, X. Y.; Baltruschat, H. *Langmuir* **2002**, *18*, 4659.
(42) Massong, H.; Wang, H. S.; Samjeske, G.; Baltruschat, H. *Electrochim. Acta* **2000**, *46*, 701.
(43) Babu, P. K.; Kim, H. S.; Oldfield, E.; Wieckowski, A. *J. Phys. Chem. B* **2003**, *107*, 7595.
(44) Babu, P. K.; Kim, H.-S.; Kuk, S. T.; Chung, J. H.; Oldfield, E.; Smotkin, E. S.; Wieckowski, A. *J. Phys. Chem. B* **2005**, in press.
(45) Dubau, L.; Hahn, F.; Coutanceau, C.; Leger, J. M.; Lamy, C. *J. Electroanal. Chem.* **2003**, *554*, 407.
(46) Park, S.; Wieckowski, A.; Weaver, M. J. *J. Am. Chem. Soc.* **2003**, *125*, 2282.
(47) Christensen, P. A.; Jin, J. M.; Lin, W. F.; Hammett, A. *J. Phys. Chem. B* **2004**, *108*, 3391.
(48) Koponen, U.; Peltonen, T.; Bergelin, M.; Mennola, T.; Valkiainen, M.; Kaskimies, J.; Wasberg, M. *J. Power Sources* **2000**, *86*, 261.
(49) Cao, D. X.; Bergens, S. H. *J. Electroanal. Chem.* **2002**, *533*, 91.
(50) Cao, D. X.; Bergens, S. H. *Electrochim. Acta* **2003**, *48*, 4021.
(51) Crabb, E. M.; Ravikumar, M. K.; Thompsett, D.; Hurford, M.; Rose, A.; Russell, A. E. *Phys. Chem. Chem. Phys.* **2004**, *6*, 1792.
(52) Petukhov, A. V.; Akemann, W.; Friedrich, K. A.; Stimming, U. *Surf. Sci.* **1998**, *404*, 182.
(53) Seiler, T.; Savinova, E. R.; Friedrich, K. A.; Stimming, U. *Electrochim. Acta* **2004**, *49*, 3927.
(54) Chrzanowski, W.; Wieckowski, A. In *Interfacial Electrochemistry: Theory, Experiment, and Applications*; Wieckowski, A., Ed.; Marcel Dekker: New York, 1999; p 937.
(55) Lee, C. E.; Bergens, S. H. *J. Phys. Chem. B* **1998**, *102*, 193.
(56) Kardash, D.; Korzeniewski, C.; Markovic, N. *J. Electroanal. Chem.* **2001**, *500*, 518−523.
(57) Lu, G.-Q.; White, J. O.; Wieckowski, A. *Surf. Sci.* **2004**, *564*, 131−140.
(58) Koper, M. T. M.; Lukkien, J. J.; Jansen, A. P. J.; van Santen, R. A. *J. Phys. Chem. B* **1999**, *103*, 5522.
(59) Frelink, T.; Visscher, W.; vanVeen, J. A. R. *Langmuir* **1996**, *12*, 3702.
(60) Cappadonia, M.; Schmidberger, J.; Schwegle, W.; Stimming, U. In *The Proceedings of the 189th Meeting of the Electrochemical Society*: Los Angeles, 1996.
(61) Strbac, S.; Johnston, C. M.; Lu, G.-Q.; Crown, A.; Wieckowski, A. *Surf. Sci.* **2004**, *573*, 80−99.
(62) Spendelow, J. S.; Wieckowski, A. *Phys. Chem. Chem. Phys.* **2004**, *6*, 5094−5118.
(63) Vericat, C.; Wakisaka, M.; Haasch, R.; Bagus, P. S.; Wieckowski, A. *J. Solid State Electrochem.* **2004**, *8*, 794−803.
(64) Feliu, J. M.; Fernandezvega, A.; Aldaz, A.; Clavilier, J. *J. Electroanal. Chem.* **1988**, *256*, 149.
(65) Clavilier, J.; Feliu, J. M.; Aldaz, A. *J. Electroanal. Chem.* **1988**, *243*, 419.
(66) Vukovic, M.; Valla, T.; Milun, M. *J. Electroanal. Chem.* **1993**, *356*, 81.
(67) Lu, G. Q.; Crown, A.; Wieckowski, A. *J. Phys. Chem. B* **1999**, *103*, 9700−9711.
(68) Lee, C. E.; Tiege, P. B.; Xing, Y.; Nagendran, J.; Bergens, S. H. *J. Am. Chem. Soc.* **1997**, *119*, 3543−3549.
(69) Lee, C. E.; Bergens, S. H. *J. Electrochem. Soc.* **1998**, *145*, 4182−4185.
(70) Gasteiger, H. A.; Markovic, N.; Ross, P. N.; Cairns, E. J. *J. Electrochem. Soc.* **1994**, *141*, 1795−1803.
(71) Dubau, L.; Coutanceau, C.; Garnier, E.; Leger, J. M.; Lamy, C. *J. Appl. Electrochem.* **2003**, *33*, 419−429.
(72) Funtikov, A. M.; Stimming, U.; Vogel, R. *J. Electroanal. Chem.* **1997**, *428*, 147.
(73) Hadzijordanov, S.; Angersteinkozlowska, H.; Vukovic, M.; Conway, E. *J. Phys. Chem.* **1977**, *81*, 2271.
(74) El-Aziz, A. M.; Kibler, L. A. *Electrochem. Commun.* **2002**, *4*, 866.
(75) Brankovic, S. R.; Marinkovic, N. S.; Wang, J. X.; Adzic, R. R. *J. Electroanal. Chem.* **2002**, *532*, 57.
(76) Jusys, Z.; Schmidt, T. J.; Dubau, L.; Lasch, K.; Jorissen, L.; Garche, J.; Behm, R. J. *J. Power Sources* **2002**, *105*, 297.
(77) Spendelow, J. S.; Lu, G. Q.; Kenis, P. J. A.; Wieckowski, A. *J. Electroanal. Chem.* **2004**, *568*, 215−224.
(78) Herrero, E.; Franaszczuk, K.; Wieckowski, A. *J. Phys. Chem.* **1994**, *98*, 5074−5083.
(79) Watanabe, M.; Zhu, Y. M.; Igarashi, H.; Uchida, H. *Electrochemistry* **2000**, *68*, 244.
(80) de Mongeot, F. B.; Scherer, M.; Gleich, B.; Kopatzki, E.; Behm, R. J. *Surf. Sci.* **1998**, *411*, 249.
(81) Tong, Y. Y.; Rice, C.; Wieckowski, A.; Oldfield, E. *J. Am. Chem. Soc.* **2000**, *122*, 11921−11924.
(82) Lu, C.; Masel, R. I. *J. Phys. Chem. B* **2001**, *105*, 9793.
(83) Lu, C.; Rice, C.; Masel, R. I.; Babu, P. K.; Waszczuk, P.; Kim, H. S.; Oldfield, E.; Wieckowski, A. *J. Phys. Chem. B* **2002**, *106*, 9581−9589.
(84) Ross, P. N. In *Electrocatalysis*; Ross, P. N., Ed.; Wiley-VCH: New York, 1998; pp 43−74.
(85) Hamnett, A. In *Interfacial Electrochemistry: Theory, Experiment, and Applications*; Wieckowski, A., Ed.; Marcel Dekker: New York, 1999; p 843.
(86) Ianniello, R.; Schmidt, V. M.; Stimming, U.; Stumper, J.; Wallau, A. *Electrochim. Acta* **1994**, *39*, 1863.
(87) Lin, W. F.; Iwasita, T.; Vielstich, W. *J. Phys. Chem. B* **1999**, *103*, 3250.
(88) Zou, S. Z.; Villegas, I.; Stuhlmann, C.; Weaver, M. J. *Electrochim. Acta* **1998**, *43*, 2811.
(89) Gomer, R. *Rep. Prog. Phys.* **1990**, *53*, 917.
(90) Viswanathan, R.; Hou, G. Y.; Liu, R. X.; Bare, S. R.; Modica, F.; Mickelson, G.; Segre, C. U.; Leyarovska, N.; Smotkin, E. S. *J. Phys. Chem. B* **2002**, *106*, 3458−3465.
(91) Hayden, B. E. In *Catalysis and Electrocatalysis at Nanoparticle Surfaces*; Vayenas, C. G., Ed.; Marcel Dekker: New York, 2003; p 171.
(92) Hammer, B.; Nielsen, O. H.; Norskov, J. K. *Catal. Lett.* **1997**, *46*, 31.
(93) Koper, M. T. M.; Lebedeva, N. P.; Hermse, C. G. *Faraday Discuss.* **2002**, *121*, 301.
(94) Lebedeva, N. P.; Koper, M. T. M.; Feliu, J. M.; Van Santen, R. A. *J. Phys. Chem. B* **2002**, *106*, 12938.
(95) Maillard, F.; Eikerling, M.; Cherstiouk, O. V.; Schreier, S.; Savinova, E. R.; Stimming, U. *Faraday Discuss.* **2004**, *125*, 357.
(96) Barth, J. V. *Surf. Sci. Rep.* **2000**, *40*, 75.
(97) He, Y. F.; Borguet, E. *Faraday Discuss.* **2002**, *121*, 17−25.
(98) Ma, J. W.; Cai, L.; Xiao, J. D.; Loy, M. M. T. *Surf. Sci.* **1999**, *425*, 131.
(99) Bercerra, L. R.; Klug, C. A.; Slichter, C. P.; Sinfelt, J. H. *J. Phys. Chem.* **1993**, *97*, 12014.
(100) Koper, M. T. M.; Shubina, T. E.; van Santen, R. A. *J. Phys. Chem. B* **2002**, *106*, 686.
(101) Tong, Y. Y.; Oldfield, E.; Wieckowski, A. *Faraday Discuss.* **2002**, *121*, 323.
(102) Maillard, F.; Savinova, E. R.; Simonov, P. A.; Zaikovskii, V. I.; Stimming, U. *J. Phys. Chem. B* **2004**, *108*, 17893.
(103) Cao, D.; Lu, G.-Q.; Wieckowski, A.; Wasileski, S. A.; Neurock, M. *J. Phys. Chem. B* **2005**, *109*, 11622.